A Real-Time Approach to Achieve Maximal Autonomy of Autonomous Underwater Vehicles in the Presence of Perturbing Flow Field

Mario A. Jordán [1,2] and Jorge L. Bustamante[1,2]

[1] Argentinean Institute of Oceanography (IADO-CONICET).
Florida 8000, Complejo CCT,
Edificio E1, B8000FWB, 8000 Bahía Blanca, ARGENTINA.

[2] Dto. Ingeniería Eléctrica y de Computadoras- Univ. Nac. del Sur
(DIEC-UNS).

Abstract. In this paper a preliminary study of optimal energy systems for autonomous underwater vehicles is presented. A method is developed for achieving maximal autonomy. A general algorithm was developed for the navigation in 6 degrees of freedom in a non-conservative flow field. It is shown that missions with selective starting point beginning with the direction of the flow are much more favorable for the autonomy.
Key words: Optimal energy spent - Unmanned underwater vehicles - AUVs - Dynamic optimization

1 Introduction

Large cruise velocities in marine systems implies high energy consumptions. This is particularly more accentuated in subaquatic vehicles in where the motion resistance force increases about proportional to the square of the velocity. Moreover, this could be critical in autonomous underwater vehicles which are powered with onboard batteries and has to cover large distances without the possibility to recharge them.

The demand of a energy from a closed energy system to propel the vehicle has to be taken into consideration as a critical factor in a mission when long mission times or large paths are specified.

Some authors like [1] have posed the problem in the context of Maximum Principle of Pontryagin. From a trajectory design point of view with the goal to design a control strategy that minimizes the energy consumption of the vehicle along a trajectory. Even if these trajectories can be theoretically be computed for a given set of initial and final configurations, unfortunately they are not implementable onto a real vehicle due to multiple and rapid switching required by the thrusters.

One can also obtain substantially energy savings by actuating only a reduced set of motors [1] or bypassing adverse currents and also exploiting favorable currents [2]. Moreover, some approaches deal directly with the dynamics equation for choosing trajectories such that hydrodynamic drag on the system is reduced

[3]. Other approaches generates directly the speed along the path based on casts of the ocean currents and a cost function containing information of inertia to speed up the convergence to the global minimum [4].

Our goal is to generate an optimal rate along a path that takes the vehicle from its starting location to a mission-specified destination, while minimizing the demanded energy cost. The proposed algorithm can make AUV travel longer and save more energy comparing to tradition path planning methods.

2 Problem statement

We will posse the problem of energy consumption and vehicle autonomy in a path-tracking problem that combines the interaction of the vehicle dynamics with the energy-source dynamics and the emergence of persistent perturbations. Here the goal is described as

Initial conditions :

- Given a high-performance control system for guidance of the vehicle dynamics and rejection of perturbations,
- the dynamics of the energy source (here batteries),
- an unknown uniform flow field $\mathbf{v}_c$ (ocean current),
- an initial battery energy value $E_0 > 0$,
- a final battery energy value E_e with $E_0 > E_e \geq 0$,
- an arbitrarily shaped and continuous spacial reference path $\boldsymbol{\eta}_{ref}(x, y, z)$ with large extension L,

Goal :

- then, one is interested in computing full battery energy E_0 up to empty out the energy to the low level E_e.

Since we are thinking in a control system with eventual unpredictable perturbations, solutions would have to be obtained in real time.

It is worth noticing that in our context $\boldsymbol{\eta}(x, y, z)$ is assumed to be fixed and the flow field may act favorably for the motion in some stretches along the path, as well as unfavorably in other ones.

2.1 Vehicle dynamics

Let the dynamics of a vehicle with 6 degrees of freedom be characterized as usually by [5]-[6]

$$\dot{\mathbf{v}} = (M_b + M_a)^{-1} \left(-C(\mathbf{v})\mathbf{v} - D(|\mathbf{v}|)\mathbf{v} + \mathbf{g}(\boldsymbol{\eta}) + \boldsymbol{\tau}_c + \boldsymbol{\tau} \right) \tag{1}$$

$$\dot{\boldsymbol{\eta}} = J(\boldsymbol{\eta})(\mathbf{v} + \mathbf{v}_c). \tag{2}$$

Herein $\boldsymbol{\eta}$ is the generalized position in an earth-fixed frame where $\boldsymbol{\eta} = [x, y, z, \phi, \theta, \psi]^T$ describes translations x, y, z along the axis, and rotations about these axes ϕ, θ, ψ, respectively; $\mathbf{v}$ is the generalized velocity vector in a vehicle-fixed frame where $\mathbf{v} = [u, v, w, p, q, r]^T$ describes the modes of motion surge, sway, heave, pitch, roll and yaw, respectively; and $\mathbf{v}_c$ is the flow vector of the surrounding fluid. Moreover M_b is the inertia matrix of the body and M_a is the additive mass of the surrounding fluid, C the Coriolis matrix, D the drag matrix, $\mathbf{g}$ is the net buoyancy vector, $\boldsymbol{\tau}_c$ the cable force (in ROV) and $\boldsymbol{\tau}$ the thruster force considered as the system input. Finally $J(\boldsymbol{\eta})$ is the well-known rotation matrix depending on the Euler angles ϕ, θ and ψ.

2.2 Autonomous navigation system

The path tracking problem is performed by an autonomous navigation system whose elements are described in the Fig. 1. The controller build up a thrust $\boldsymbol{\tau}$ according to a feedback of the spatial states in $\boldsymbol{\eta}$ and kinematic states in $\mathbf{v}$. Accordingly reference trajectories for the geometric path $\boldsymbol{\eta}_{ref}$ and the desired cruise velocity $\mathbf{v}_{ref}$ along it are specified beforehand. The controller output $\boldsymbol{\tau}$ feeds an additional algorithm constructed upon a model of the inverse dynamics of the actuators and generates desired rpm's of the thrusters $\mathbf{n}_{ref}$ to diminish the path errors $\tilde{\boldsymbol{\eta}}$ and $\tilde{\mathbf{v}}$. Often this dynamics is assumed parasitics faced with the dominant dynamics of the vehicle.

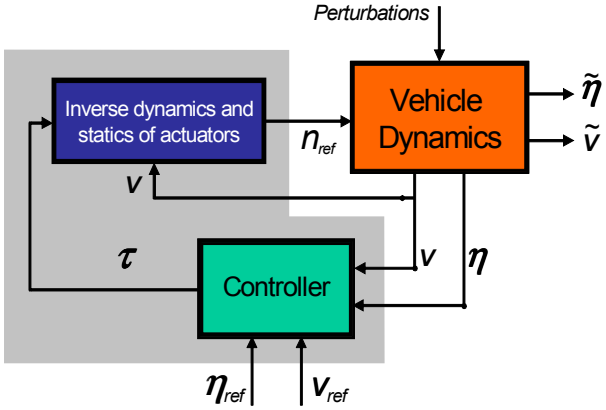

Fig. 1 - Control system for tracking of geometric and kynematic reference trajectories

Inertial and/or kinematic perturbations are also possible, for instance, mass changes and fluid flow.

It is assumed that the controller is able to force the errors $\tilde{\boldsymbol{\eta}}$ and $\tilde{\mathbf{v}}$ to zero asymptotically with any references provided that the acceleration $\dot{\mathbf{v}}_{ref}(t)$ is continuous.

Moreover in this paper, a high-performance controller is design upon a good model of the system and works in such a way that path errors $\tilde{\boldsymbol{\eta}}$ and $\tilde{\mathbf{v}}$ go rapidly to null and the dynamics of the control system is simple. One design that possesses these features is developed in [7].

Accordingly to this work, the error system of the open-loop dynamics is

$$\dot{\tilde{\boldsymbol{\eta}}} = -K_p\tilde{\boldsymbol{\eta}} + J\tilde{\mathbf{v}} + J\,\mathbf{v}_c \tag{3}$$

$$\dot{\tilde{\mathbf{v}}} = -M^{-1}(C+D)\left(\tilde{\mathbf{v}} + J^{-1}\left(\dot{\boldsymbol{\eta}}_{ref} - K_p\tilde{\boldsymbol{\eta}}\right)\right) - M^{-1}\mathbf{g} - \frac{d\left(J^{-1}\dot{\boldsymbol{\eta}}_{ref}\right)}{dt} + \\ + \dot{J}^{-1}K_p\tilde{\boldsymbol{\eta}} + + J^{-1}K_p\left(J\tilde{\mathbf{v}} - K_p\tilde{\boldsymbol{\eta}} + J\,\mathbf{v}_c\right) + M^{-1}\boldsymbol{\tau}$$

with the tracking errors

$$\breve{\boldsymbol{\eta}}=\boldsymbol{\eta}-\boldsymbol{\eta}_{ref} \tag{4}$$

$$\breve{\mathbf{v}}=\mathbf{v}-J^{-1}(\boldsymbol{\eta})J(\boldsymbol{\eta}_{ref})\mathbf{v}_{ref}+J^{-1}(\boldsymbol{\eta})K_p\breve{\boldsymbol{\eta}}, \tag{5}$$

the feedback vector (thrust)

$$\begin{aligned}\boldsymbol{\tau}=&C\mathbf{v}+D\mathbf{v}+\mathbf{g}+ \\ &+M\left(\frac{d}{dt}(J^{-1}(\boldsymbol{\eta})\dot{\boldsymbol{\eta}}_{ref})-\frac{dJ^{-1}(\boldsymbol{\eta})}{dt}K_p\breve{\boldsymbol{\eta}}+J^{-1}(\boldsymbol{\eta})K_p^2\breve{\boldsymbol{\eta}}-J^{-1}(\boldsymbol{\eta})K_pJ(\boldsymbol{\eta})\breve{\mathbf{v}}\right)- \\ &-K_v\breve{\mathbf{v}}-J^T\breve{\boldsymbol{\eta}}.\end{aligned} \tag{6}$$

By feedbacking this control thrust with neglected thruster dynamics in the open-loop system, the error system of Fig. 1 results in

$$\dot{\breve{\boldsymbol{\eta}}} = -K_p\breve{\boldsymbol{\eta}}+J\breve{\mathbf{v}}+J\ \mathbf{v}_c \tag{7}$$

$$\dot{\breve{\mathbf{v}}} = -M^{-1}K_v\breve{\mathbf{v}}-M^{-1}J^T\breve{\boldsymbol{\eta}}+J^{-1}K_pJ\mathbf{v}_c. \tag{8}$$

$$\mathbf{n}_{ref} = \mathbf{f}(\boldsymbol{\tau},\mathbf{v}). \tag{9}$$

where $\mathbf{f}$ is a nonlinear function describing the static characteristic of the thrusters.

It is noticing that the flow field appears as perturbation in (7) and (8). The additional push or braking given by the flow field $\mathbf{v}_c$ to the vehicle is compensated by the controller, which doses the energy taken from the battery conveniently in order to maintain the references for course and cruise velocity.

2.3 Energy balance

The total energy available for the navigation is supplied internally by the batteries and externally by the motion fluid in the vehicle surroundings due to an eventual flow field.

As the system is fully controlled, it is difficult to evaluate the energy contribution between these sources during the navigation. Certainly, when the flow pushes the vehicle, the controller takes from the battery a minimal amount of energy, while in the worst case of counter-flow, the controller must take much more energy from the battery in order to compensate the emerging drag. This evaluation would require the computation of the battery energy in two different flow conditions of path tracking, namely with $\mathbf{v}_c{\neq}0$ and with $\mathbf{v}_c{=}0$.

So, the control system determines the available energy for the navigation which is just the energy in the batteries

$$E_b(t) = E_0 - \int_{t_0}^{t} i_b\ V_b\ d\tau = E_m + E_{ns} + E_{lb} + E_t \tag{10}$$

with i_b the supplied current and V_b the voltage. The partial energies of E_b are

$$E_m(t) = \int_0^{\mathbf{s}(t)} \boldsymbol{\tau}^T\ d\mathbf{s}= \int_0^t \boldsymbol{\tau}^T\ \mathbf{v}dt' \text{ with } \mathbf{v}_c{=}0 \tag{11}$$

$$E_{ns}(t) = \int_0^t p_{ns}dt' = \bar{p}_{ns}\ t \tag{12}$$

$$E_{lb}(t) = E_0 - \alpha_b \int_0^t 1 \; dt' = E_0 - \frac{\alpha_b}{2} t \tag{13}$$

$$E_t(t) = nR_a \int_0^t \mathbf{i}_a^2 \; dt, \tag{14}$$

where p_{ns} is the power needed for the operation of the navigation system which is assumed constant and equal to $\bar{p}_{ns}$, α_b is a constant representing the leakage rate per time unit in the battery, respectively, and finally, $\mathbf{i}_a$ and R_a are the current vector and the armature resistance in the n thrusters of the vehicle. The vector $\mathbf{s}(t)$ is the stretch which is run at t.

One necessary condition of the spent energy is

$$\dot{E}_b(t) < 0. \tag{15}$$

The case $\dot{E}_b(t) = 0$ has no mean since the controller and instruments are permanent energized.

The analytical evaluation of $\boldsymbol{\tau}$ in (6) is possible because expressions for M, C, D and $\mathbf{g}$ are available [5]. Also the design matrices K_p and K_v are defined in the controller design [8], while the states $\boldsymbol{\eta}$ and $\mathbf{v}$ are measured and so the rotation matrix $J(\boldsymbol{\eta})$ can be calculated.

3 Dynamic optimization for maximal autonomy

The optimization solution can be described by an optimal trajectory accomplishing

$$E_{b_{OPT}}(t) = \underset{\substack{L=L_{\max} \\ \text{with } \dot{E}_b(t)<0 \\ L=0 \rightarrow E_b=E_0 \text{ and } L=L_{\max} \rightarrow E_b=E_e<E_0}}{\text{optim}} E_b\left(t, \boldsymbol{\eta}_{ref}(t), \mathbf{v}_c(t)\right). \tag{16}$$

The profile (16) is optimal in the sense that each variation $\delta E_b(t)$ around $E_{b_{OPT}}(t)$ with the conditions $\delta \dot{E}_b(t) \leq 0$ and $\delta E_b(0) = \delta E_b(L_{\max}) = 0$, will produce a suboptimal autonomy L, with $L < L_{\max}$.

Possible real solutions are illustrated in Fig. 2.

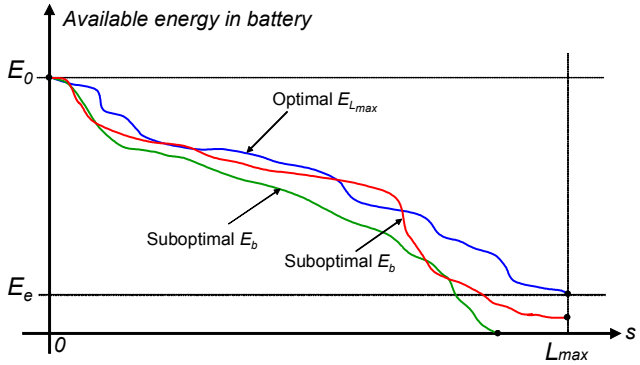

Fig. 2 - Optimal and suboptimal spent of energy in a stipulated time T in order for the vehicle to achieve maximal run length $L_{\max}$

It is worth noticing in (16) that the only way to manipulate the energy-spent trajectory is the assignation of the parameter time in the spatial coordinates and then establishing the desired rhythm of navigation, it is

$$\boldsymbol{\eta}_{ref}(t) \rightarrow \mathbf{v}_{ref}(t) = J^{-1}(\boldsymbol{\eta}_{ref})\dot{\boldsymbol{\eta}}_{ref}(t) \rightarrow \mathbf{s}(t) = \int_0^t \mathbf{v}_{ref}(t')dt' \tag{17}$$

In this way, the rhythm of advance is actually given by the vector function $\mathbf{s}(t)$, which can be illustrated as a point that runs along the path with velocity equal to $\mathbf{v}_{ref}(t)$.

Before introducing the method to find the optimal solution analytically, we have to discussed the influence of both the flow field $\mathbf{v}_c$ and the transients in the control system.

3.1 Influence of flow fields on energy spent

As seen in (11), the energy spent in mechanic motion was indicated for null flow field $\mathbf{v}_c$. In fact, the corresponding spent energy E_m can be calculated directly according to (11) by means of the control law generated by the controller in (6).

The influence of $\mathbf{v}_c$ upon the optimal decay law $E_{b_{OPT}}(t)$ can intuitively be checked easily as follows. Clearly, when $\mathbf{v}_c^T\mathbf{v}>0$, the consumption power of the battery would be smaller in time than in the case with $\mathbf{v}_c=0$ because of the favorable drag. Additionally, it would be much more small in the counter-flow case, it is when $\mathbf{v}_c^T\mathbf{v}<0$, because of the motion resistance.

As the influence of $\mathbf{v}_c$ is not considered in $\boldsymbol{\tau}$ we must modify the energy component E_m. So, an analytic expression for the modified E_m is

$$E_{m_{v_c}}(t) = \int_0^t \boldsymbol{\tau}_{v_c}^T \mathbf{v}\, dt', \tag{18}$$

with

$$\begin{aligned}\boldsymbol{\tau}_{v_c} = & C(\mathbf{v}-\mathbf{v}_c) + D(\mathbf{v}-\mathbf{v}_c) + \mathbf{g} + M\left(\frac{d}{dt}(J^{-1}(\boldsymbol{\eta})\dot{\boldsymbol{\eta}}_{ref}) - \frac{dJ^{-1}(\boldsymbol{\eta})}{dt}K_p\tilde{\boldsymbol{\eta}} + \right. \\ & \left. + J^{-1}(\boldsymbol{\eta})K_p^2\tilde{\boldsymbol{\eta}} - J^{-1}(\boldsymbol{\eta})\, K_p J(\boldsymbol{\eta})\left(\tilde{\mathbf{v}}-\mathbf{v}_c\right)\right) - K_v\left(\tilde{\mathbf{v}}-\mathbf{v}_c\right) - J^T\tilde{\boldsymbol{\eta}}.\end{aligned} \tag{19}$$

Here $\mathbf{v}_c$ is unknown and must be estimated so that (19) can be calculated.

This end is achieved from the total energy consumed by the thruster system. Thus

$$E_{m_{v_c}}(t) = nV_a \int_0^t \sum_{i=1}^{n} |i_{a_i}|\ dt' - nR_a \int_0^t \mathbf{i}_a^2\ dt', \tag{20}$$

where V_a is the source voltage of the thrusters and i_{a_i} the armature current of each thruster. Here $\mathbf{i}_a$ is measurable and R_a is known. Thus, combining (19) in (18) and (20), it is generally possible to estimate $\mathbf{v}_c$.

However, a practical way to calculate $\mathbf{v}_c$ directly is based on the following assumption. Since we are considering only high-performance controllers, we can think $\tilde{\boldsymbol{\eta}}=\tilde{\mathbf{v}}=0$ after a short transient. So in steady state it is valid

$$\boldsymbol{\tau}_{v_c}=C\left(\mathbf{v}-\mathbf{v}_c\right)+D\left(\mathbf{v}-\mathbf{v}_c\right)+\mathbf{g}+K_v\mathbf{v}_c+ \tag{21}$$
$$+M\left(\frac{d}{dt}(J^{-1}(\boldsymbol{\eta}_{ref})\dot{\boldsymbol{\eta}}_{ref})+J^{-1}(\boldsymbol{\eta}_{ref})\ K_pJ(\boldsymbol{\eta}_{ref})\mathbf{v}_c\right)$$

and $\mathbf{v}_c$follows much more easily from combining (21) in (18) and (20).

3.2 Lost energy due to controller transients

The effects of uniform perturbations on the vehicle appearing as drag from the flow field, can usually be attenuated by the control system. However, when the vehicle navigates according to such a paths $\boldsymbol{\eta}(x,y,z)$ that proposes changes of course intermittently, the drag will act from different directions. Thus, in these situations, the controller has to deal with abrupt changes of perturbation.

As the controller has a wide frequency band, we can assume the power consumed by the thrusters occurs in short times referred to as ΔT. Therefore the energy of the battery decays suddenly. So we can model the total lost energy during a transient from the battery current as

$$\Delta E_{b_{trans}}(t)=E_b(t+\Delta t)-E_b(t)=V_b\int_t^{t+\Delta T} i_{lb}\ dt'. \tag{22}$$

Clearly, this short time ΔT is seen in the large navigation period as differential increment of time, and the power in the transient as an impulse. The consequence is that E_b is not continuous in time.

Of course, the evaluation of $\Delta E_{b_{trans}}$ implies a permanent monitoring of E_b in time.

3.3 Introductory method without field flow

We introduce the key idea of our optimization method through a simple case study before we can straightforwardly generalize it.

Let the underwater vehicle be fully controlled. Moreover, suppose the battery energy flows to satisfy demands of the instrument and of the motion to overcome the quadratic drag in a rectilinear motion. Additionally, the warm generated in battery and thrusters is neglected. So the available energy at any time point t is (see (12) and (11))

$$E(t)=E_0-E_{ns}(t)-E_m(t)= \tag{23}$$
$$=E_0-\bar{p}_{ns}t-\int_0^t c\,|v|\,v^2\ dt'. \tag{24}$$

Now suppose we are searching a reference velocity $\mathbf{v}_{ref}$ for reaching maximal autonomy of the vehicle starting with the battery energy E_0 up to completely empty the battery, it is $E_e=0$.

Additionally we think to define a finite number of constant velocities $\mathbf{v}_{ref}$, changed arbitrarily in stretches of the path $\boldsymbol{\eta}(x)$. We begin with $\mathbf{v}_{ref}^T=[u_{ref},0,0,0,0,0]^T=u_0$ up to achieve some arbitrary energy level $E_1<E_0$. Also, let us suppose there is no flow. So we have

$$E(T)=E_1=E_0-\bar{p}_{ns}T-cu_0^3T \tag{25}$$

$$T = \frac{E_0 - E_1}{\bar{p}_{ns} + cu_0^3} \text{ and } L = u_0 \frac{E_0 - E_1}{\bar{p}_{ns} + cu_0^3}. \tag{26}$$

For an extreme we search

$$\frac{\partial L}{\partial u_0} = \frac{(E_0 - E_1)\left(\bar{p}_{ns} - 2cu_0^3\right)}{\left(\bar{p}_{ns} + cu_0^3\right)^2} = 0. \tag{27}$$

$$\text{So, it results } u_0 = \sqrt[3]{\frac{\bar{p}_{ns}}{2c}} \text{ and} \tag{28}$$

$$L_{\max 1} = (E_0 - E_1)\sqrt[3]{\frac{4}{27c\bar{p}_{ns}^2}}. \tag{29}$$

Now we propose to find a second velocity u_1 to cover the path with maximal autonomy up to fully empty the battery from the last level E_1. Using (29) we find surprisingly $u_0 = u_1$ and the maximal autonomy equal to $L_{\max} = L_{\max 1} + L_{\max 2} = E_0 \sqrt[3]{\frac{4}{27c\bar{p}_{ns}^2}}$. The result would be also optimal if we had considered linear instead quadratic drag.

This first result says us that no matter how large the number of velocities we allow to be involved in the optimization process, the result will be always the same, it is, that only one velocity is necessary for achieving a maximal autonomy $L_{\max}$ from arbitrary defined two energy levels.

3.4 Introductory method with field flow

Intuitively, the scene must be different when a flow field does exist because the fluid current may extract energy from the battery while the path tracking control forces path errors to go to zero or, on the contrary, may provide energy for the motion alleviating the battery.

So we think through a collinear flow field with $\mathbf{v}_c$ which is first positive v_c during a specified period T and subsequently negative $-v_c$ in another period T of the same duration. Suppose E_0 is sufficiently large such that the battery does not go empty after $2T$. The flow rate v_c can be detected and calculated by combining (21) and (20).

In the first period T, the energy declines from E_0 up to E_1 corresponding to a specified period T. From $\frac{\partial L}{\partial u_0} = 0$ one obtains the condition $\bar{p}_{ns} - 2cv^3 + c3v^2 v_c = 0$, which has only one real root as it can be verified from the discriminant condition $\Delta = -\left(\frac{v_c^3}{8}\right)^2 + \left(\frac{\bar{p}_{ns}}{4c} + \frac{v_c^3}{8}\right)^2 > 0$ for $v_c > 0$. The optimal velocity in this first period is

$$u_{0_1} = \sqrt[3]{r + \sqrt[2]{q^3 + r^2}} + \sqrt[3]{r - \sqrt[2]{q^3 + r^2}} + \frac{v_c}{2} \tag{30}$$

$$r = \frac{\bar{p}_{ns}}{4c} + \frac{v_c^3}{8} \quad \text{and} \quad q = -\frac{v_c^2}{4}.$$

Afterwards, in the second period T, the polynomial is $\bar{p}_{ns} - 2cv^3 - c3v^2 v_c = 0$ for $v_c < 0$. The discriminant condition $\Delta = -\left(\frac{v_c^3}{8}\right)^2 + \left(\frac{\bar{p}_{ns}}{4c} + \frac{v_c^3}{8}\right)^2 < 0$ says that there exist three real roots, but only one positive. This is

$$u_{0_2} = -\frac{v_c}{2} > 0. \tag{31}$$

Analyzing (30) and (31) one can draw out

$$u_{0_1} > u_{02} + 2\,|v_c| \tag{32}$$

which implies a result that was expected

$$(u_{0_1} - v_c)\,T > (u_{0_2} + v_c)\,T \tag{33}$$

$$L_{\max_1} > L_{\max_2} \tag{34}$$

We can deduce now one new result which is meaningful for applications in navigation of AUVs. Suppose the start energy E_0 has such a low value so that within the second period T the battery energy goes to null. Here, we can distinguish two scenes: 1) the vehicle undergoes $v_c > 0$ during T and then $v_c < 0$ during $T_1 < T$; 2) the vehicle undergoes $v_c < 0$ during T and then $v_c > 0$ during $T_2 < T$. Clearly, the vehicle stops before ending $2T$. This means that the following condition is valid $E_0 - (2\bar{p}_{ns} + c\overset{3}{u_{0_1}} + c\overset{3}{u_{0_2}})T < 0$.

If we calculate the duration of the second periods, one gets

$$L_{\max_{T+T_1}} = (u_{0_1} - v_c)\,T + \frac{E_0 - (\bar{p}_{ns} + c\overset{3}{u_{0_1}})T}{(\bar{p}_{ns} + cu_{0_2}^3)}\,(u_{0_2} + v_c) \tag{35}$$

$$L_{\max_{T+T_2}} = (u_{0_2} + v_c)\,T + \frac{E_0 - (\bar{p}_{ns} + c\overset{3}{u_{0_2}})T}{(\bar{p}_{ns} + cu_{0_1}^3)}\,(u_{0_1} - v_c)\,. \tag{36}$$

Since $u_{0_1} > u_{02} + 2\,|v_c|$, it results $L_{\max_{T+T_1}} > L_{\max_{T+T_2}}$.

This last result signifies that if the vehicle has to navigate bidirectionally from a launching point up to exhausting the battery, first going in favor of the flow and then returning in counter-low sense, it achieves a larger autonomy than in the case of starting first in counter-flow direction and then of returning to the launching point.

3.5 Application

So we find out that the flow field is not conservative. This is illustrated in Fig. 3 on the top. This means, if the vehicle begins its trajectory through the way A and turns around the rectangle, it will accomplish a larger autonomy than in the case if it decides on the way B.

Moreover, if an AUV is launched from a ship to go and return rectilinearly from a start point (see Fig. 3, bottom), it will achieve less consume of energy if it runs from A to B and return to A than in the contrary case, it is, it would have to be launched at best from A.

4 Generalized method

We can generalize our introductory methods for an autonomous navigation controller system like the one in Fig. 1, and state an arbitrary reference path in 6 degrees of freedom and the whole vehicle dynamics.

In this way, we can deal with all spent energies during navigation (11)-(14) E_m, E_{ns}, E_{lb} and E_t. Also transient in any combination of motions are included, and finally the non-conservative flow field is taken into account.

The goal is to determine the autonomy vector $\mathbf{L}$ and the rate reference $\mathbf{v}_{ref}(t)$ in the presence of perturbations of a uniform flow field and transients.

We will work an algorithm out that contains following steps:

1 Define the path $\boldsymbol{\eta}(x, y, z)$,

2 Define the starting and final energies E_0 and E_e,

3 Specify analytical expressions for $E_b(t) = E_m + E_{ns} + E_{lb} + E_t$ according to (18) and (12)-(14),

4 Estimate $\mathbf{v}_c$ from (21) and (20),

5 Calculate $\mathbf{L}$=$\mathbf{v}_{ref}\frac{E_0-E_e}{\bar{p}_{ns}+cu_0^3}$ and the conditions $\frac{\partial \mathbf{L}}{\partial \mathbf{v}_{ref}}$=0,

6 Calculate the optimal velocity vector $\mathbf{v}_{ref}(t)$ from conditions of the step 5),

7 If some control transient occurs and/or a sudden change of the flow field takes place, calculate the energy drop $\Delta E_{b_{trans}}$ from (22) and/or the new $\mathbf{v}_c$ from the step 4). Recalculate new $\mathbf{v}_{ref}(t)$,

8 If $E_b(t) > E_e$ go to 5). Otherwise stop the vehicle.

The algorithm is implemented in a new controller for energy optimization illustrated in Fig. 4.

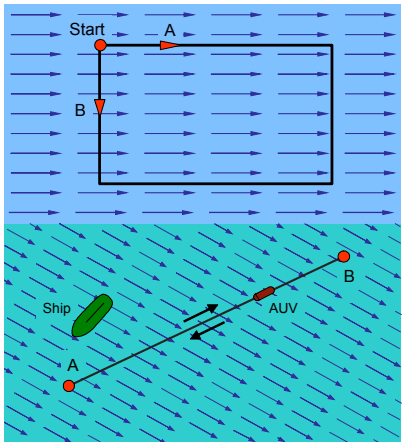

Fig. 3 - Top: Non-conservative flow field. Bottom: Convenient path for maximal autonomy: $\overline{\text{A-B-A}}$

4.1 Case study

We focus a case study with following setup

$$E_0 = 1728 \text{ (KJ)} \qquad E_e = 0 \text{ (w)}$$
$$p_{ns} = 20 \text{ (w)} \qquad c = 24 \text{ (Kg/m)}$$
$$\mathbf{v}_c = \pm 0.2 \text{ (m/s)} \quad \Delta E_{trans} = 50 \text{ (KJ)}.$$

Moreover, the flow field is simulated to change periodically in opposite sequences. The changes of $\mathbf{v}_c$ produces energy drops due to control transients.

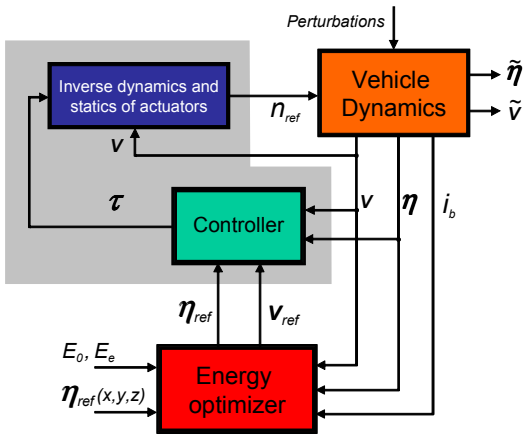

Fig. 4 - Nested control loops with energy optimizer

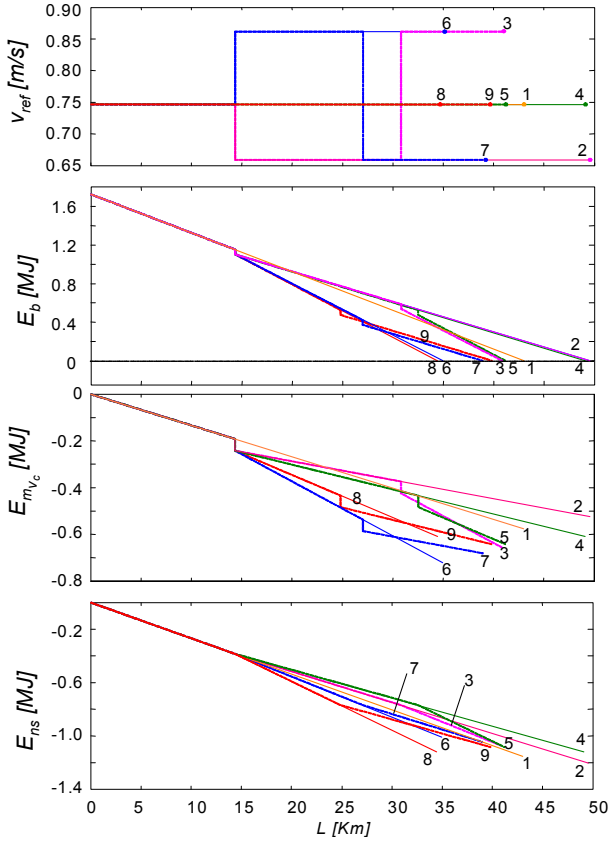

Fig. 5 - Optimal-energy curves to achieve maximal autonomy. Illustration of 9 cases

In Fig. 5 the features of the proposed algorithm are illustrated in nine cases. They are:

1) Optimal velocity curve without flow field; 2) Optimal velocity curve with favorable flow $v_c > 0$; 3) Optimal velocity curve with two changes of v_c, first positive, then negative; 4) Nonoptimal velocity curve with favorable flow v_c; 5) Nonoptimal velocity curve with two changes of v_c, first positive, then negative; 6) Optimal velocity curve with counter flow $v_c < 0$; 7) Optimal velocity curve with two changes of v_c, first negative, then positive; 8) Nonoptimal velocity curve with counter flow v_c; 9) Nonoptimal velocity curve with two changes of v_c, first negative, then positive.

It is seen that the larger autonomy is in the case 2). However one meaningful case is 4) in which it is navigate with the same velocity that was optimal before the flow might have changed. Also a comparison of cases 3) and 7) illustrates the navigation in a nonconservative flow field.

5 Conclusions

In this paper a preliminary study of optimal energy systems for autonomous underwater vehicles is presented. A method is developed for achieving maximal autonomy. A general algorithm was developed for the navigation in 6 degrees of freedom in a non-conservative flow field. It is shown that missions with selective starting point beginning with the direction of the flow are much more favorable for the autonomy. A case study has illustrated the features of the algorithm.

References

1. M. Chyba, T. Haberkorn, S.B. Singh, R.N. Smith, S.K. Choi,: Increasing underwater vehicle autonomy by reducing energy consumption. *Ocean Engineering*, 36, 62–73 (2009)
2. Kruger, D., Stolkin, R., Blum, A., Briganti, J.: Optimal AUV path planning for extended missions in complex, fast-flowing estuarine environments. In: IEEE International Conference on Robotics and Automation, Roma, 10-14 April, pp. 4265-4270 (2007)
3. Sarkar, N., Podder, T.K.: Coordinated motion planning and control of autonomous underwater vehicle-manipulator systems subject to drag optimization. *IEEE Journal of Oceanic Engineering*, 26 (2), 228-239 (2001)
4. Ge Yang, Rubo Zhang: Path Planning of AUV in Turbulent Ocean Environments Used Adapted Inertia-Weight PSO. In: Fifth International Conference on Natural Computation, ICNC '09. 14-16 Aug., pp. 299-302 (2009).
5. Fossen, T.I.: Guidance and Control of Ocean Vehicles. John Wiley&Sons, New York (1994)
6. Inzartev, A.V. (Editor): Underwater Vehicles. In-Tech, Vienna, Austria (2009).
7. Jordán, M.A., Bustamante, J.L.: Guidance of Underwater Vehicles with Cable Tug Perturbations Under Fixed and Adaptive Control Modus. *IEEE Journal of Oceanic Engineering*, 33 (4), 579- 598, (2008)
8. Jordán, M.A., Bustamante, J.L.: Adaptive Control for Guidance of Underwater Vehicles. in Underwater Vehicles, A.V. Inzartev (Editor), Chapter 14, pp. 251-278, In-Tech, Vienna, Austria (2009)